UNIVERSITY OF TARTU
FACULTY OF SCIENCE AND TECHNOLOGY
INSTITUTE OF PHYSICS

Andrei Kovaljov

MAGNETOMETRIC METHODS FOR DETECTION OF FERROMAGNETIC OBJECTS

MAGNETOMEETRILISED MEETODID FERROMAGNETILISTE OBJEKTIDE TUVASTAMISEKS

Master's thesis (30 EAP)

Supervisor:
Alan Henry Tkaczyk, Ph.D;

Tartu 2018

Table of contents

MAGNETOMETRIC METHODS FOR DETECTION OF FERROMAGNETIC OBJECTS

The first goal of this thesis was to develop method that will allow to detect automatic weapons with security portal based on work of two fluxgate magnetometers (3 axis "Mag690-100" detectors, Bartington Instruments®). The second goal was to compare work of single detector with work of single magnetometric gradiometer and to develop recommendations based on this comparison that may improve the work of the pedestrian security portal in future. On order to achieve them, following steps were made:

1. The theoretical model of a moving magnetic dipole through a security portal was made and compared with results of real experiments.
2. Various effects that may influence on results of measurements were studied and their approximate influence were evaluated.
3. Experimental setup with 2 fluxgate magnetometer detectors and various objects of interest was constructed.
4. Feasibility of using fluxgate magnetometer detectors as part of security portals operating in real time has been confirmed.
5. The work of a single detector was compared with work of gradiometer.

The results show that it is possible to detect real automatic weapons and to find their position with accuracy ±25 cm by using portal system with ordinary magnetometers. Also, it became clear that gradiometer-based security portal may decrease significantly the level of noise and thus improve the sensitivity and accuracy of the portal security system.
CERCS codes: P180, Metrology, physical instrumentation; P200, Electromagnetism, optics, acoustics.
Keywords: magnetometry, fluxgate magnetometer, gradiometer, security portal

MAGNETOMEETRILISED MEETODID FERROMAGNETILISTE OBJEKTIDE TUVASTAMISEKS

Käesoleva töö esimeseks eesmärgiks oli katseliselt välja töötada meetod, mis lubab ehitada turvalisuse portaali, mis baseerub kahe ferrosondi tööl (3-teljelised "Mag690-100" detektorid, Bartington Instruments®). Teiseks eesmärgiks oli võrrelda ühe detektori töö ühe magnetomeetrise gradiomeetri tööga ja ette valmistada nõuandeid, mis võiksid parandada turvalisuse portaali töö. Selle saavutamiseks teostati järgnev:

1. Ehitati teoreetiline mudel, mis simuleeris magnetdipooli liikumist turvalise portali läbi. Arvutustulemused said kinnitust otsemõõtmistel.
2. Uuriti erinevaid effekte, mis võivad tekitada mõju sõltuvalt erinevate eksperimentaalsete skeemide koostamisest ja määrati nende panus eksperimendi tulemustele.
3. Koostati eksperimentaalne skeem, mis koosnes kahest ferrosondi-põhilisest detektorist ning erinevatest uurimisobjektidest.
4. Tõestati ferrosondi-põhiliste detektorite sobivus kasutamiseks reaalajas töötavates turvaväravates.
5. Võrreldi üksiku detektori töö üksiku gradiomeetri tööga.

Tulemused näitavad, et on võimalik detekteerida automaatilisi relvasid ning leida nende asukoht ±25 cm täpsusega kasutades portaali süsteemi tavalise magnetomeetritega. Veel nad näitavad, et gradiomeetri-põhiline portaal võib vähendada müra tase mitu korda, ning sellepärast parandada portaali süsteemi töö.

CERCS koodid: P180, Metroloogia, instrumentatsioon; P200, Elektromagnetism, optika, akustika.
Võtmesõnad: magnetomeeteria, ferrosond, gradiomeeter, turvalisuse portaal

1. Introduction

Nowadays society is balancing between freedom and security. On the one hand, the basic need for safety is easy to understand, especially after series of terrorist's attacks. And usually people think that if there is possibility to increase the level of security, then it should be done. But on the other hand, too high level of security always means various limitations of freedom. One of the best examples for this rule are airports: 60-70 years ago it was relatively easy to get inside the airplane with gun, for example. However, after some tragic incidents with hijacking jets various countries started to improve the procedure of checking of every passenger, so nowadays it is nearly impossible to get into the airplane with gun or knife. Due to those efforts, we can travel more safely, but it also means that we have to wait much longer on the security control, which usually leads to longer queues. Same security measures and same problems may be found in a lot of places all over the world: seaports, railway stations, airports, customs and border checkpoints, etc. So, in order to decrease the time that is necessary for check-in procedure (but without significant decrease of security), new detecting systems are being developed. Depending on type of threat objects that should be detected, modern people-screening technologies are based on number fundamental chemical and physical laws and principles. The following list shows some of them [1]:

1. Metal detection
2. Chemiluminescence (CL)
3. Electron capture detectors (ECD)
4. Surface acoustic wave (SAW)
5. X-ray backscattering
6. Active microwave and millimeter-wave (mm-wave) imaging
7. Passive microwave and mm-wave imaging
8. Terahertz imaging
9. Liquid explosives screening

Depending on goals and circumstances proper type of technology is being used. The ideal security system should be able to detect any type of threat with high detection probability and low false alarm rate. It is impossible to create such a system using only one kind of technology, at least with current level of science. Thus, it is clear that such a system should include at least few different technologies that can detect the most widespread threads: metal detection (weapons), explosives detection and probably gamma radiation detection (so-called “dirty” bombs) [2], [3]. This work was done in collaboration with APSTEC Systems. It is focused only on automatic weapon detection, but its results will be applied to a real complex security system that will be able to detect all 3 basic threats that are mentioned above. [3], [4]

One of the most promising directions in the field of automatic weapon detection are magnetometers. “Magnetometer is an instrument for measuring the magnitude, direction and temporal dependence of magnetic fields and for the examination of magnetic substances.” [5]

Comparing with ordinary metal detection systems that are based on Active Electromagnetics technology (archway or handheld), magnetometers have following advantages:

1. Safety. Passive magnetometers do not emit anything, thus they will not cause any problems to people with artificial cardiac pacemakers.

2. No screening preparations. When people pass through a passive magnetometric portal, they do not need to remove a lot of objects, like jewelery, keys, mobile phones, etc. This significantly decreases time that is necessary for passing through the portal. Usually it is 4-5 times faster, up to 1000 people per hour.

3. No need for calibration. The Earth's magnetic field is already measured all over the world, and it has a constant value (this will be discussed later in Chapter 2.4).

Also, it is necessary to mention about another advanced method that may be used for automatic weapon detection. It is co/cross polarization method that is based on non-imaging mm-wave and microwave technology. Its main advantage is that this method allows to detect not only metal objects, but also dielectric objects that are concealed on a human body. [1]

However, comparing with passive magnetometry, co/cross polarization method have some serious disadvantages [1]:

1. In current real-life applications the area of detection is mainly front chest area. In means that objects that are hidden in back, legs or hands area have pretty high chances to pass through the detection system without being noticed.

2. If the threat object is being shielded by another human or aluminum foil, then there is also a high probability for threat object to stay unnoticed.

3. It has low performance to flat metallic surface of weapon attached to body at zero angle.

4. Current real-life applications are very expensive.

All those problems may be solved by using passive magnetometry. Of course, it also has its own disadvantages: magnetometers may detect only magnetized objects and there is necessity for background study, before installation of detection system. The main reason of this study is a noise from various artificial objects: electrical lines, cars, machines, etc.

2 Theoretical aspects of magnetic field measurement

2.1 Maxwell equations

Maxwell equations (ME) form a keystone for of modern physics. They describe a deep relation between electrical and magnetic fields, electrical charges and currents.

The first equation from the set of ME is also known as Gauss law. It states that the flux of the electric field strength ***E*** through a closed surface *S* is equal to the total electric charge *Q* that is containing in the volume enclosed by this surface *S* divided by vacuum permittivity $\varepsilon_0 = 8.885 \cdot 10^{-12}$ F/m:

$$\oiint_S \vec{E} \cdot \vec{ds} = \frac{Q}{\varepsilon_0} \quad (1)$$

Gauss law may be also written in differential form, where ρ is the total electric charge density (charge per unit volume). Physically it means that electrical charge is the source of the of electrical field:

$$\nabla \vec{E} = \frac{\rho}{\varepsilon_0} \quad (2)$$

The second ME is also known as Gauss law for magnetic field. It states that the flux of magnetic filed ***B*** through a closed surface is equal to 0:

$$\oiint_S \vec{B} \cdot \vec{ds} = 0 \quad (3)$$

Its differential form can be written as:

$$\nabla \vec{B} = 0 \quad (4)$$

Physically it means that the elementary magnetic charge does not exist and that it is impossible to separate north and south poles of a magnet.

The third ME is also known as Maxwell-Faraday equation. It states that the voltage induced in a closed loop is proportional to the rate of change of the magnetic flux that the loop encloses. In other words, a changing in time magnetic field produces an electric field (Σ is surface, whose boundary is a wire loop):

$$\oint_{\delta\Sigma} \vec{E}\, \vec{dl} = -\left(\frac{d}{dt}\right) \iint_{\Sigma} \vec{B}\, \vec{dS} \quad (5)$$

Same equation in differential form:

$$\nabla \times \vec{E} = \frac{d}{dt} \vec{B} \quad (6)$$

The fourth ME is also known as Ampère's circuital law with Maxwell's addition. It states that the magnetic field induced around a closed loop is proportional to the sum of electric current and displacement current (rate of change of electric field) that the loop encloses:

$$\oint_{\delta\Sigma} \vec{B}\,\vec{dl} = \mu_0 \iint_{\Sigma} \vec{J}\,\vec{dS} + \mu_0 \varepsilon_0 \frac{d}{dt} \iint_{\Sigma} \vec{E}\,\vec{dS} \quad (7)$$

Same equation in differential form:

$$\nabla \times \vec{B} = \mu_0 \vec{J} + \mu_0 \varepsilon_0 \frac{d}{dt} \vec{E} \quad (8)$$

First 2 ME show us that time-independent electric and magnetic fields are completely independent from each other. But situation changes, when either electric or magnetic field becomes time-dependent. In that case, both electric and magnetic fields becomes dependent on each other. [6], [7]

2.2 Magnetic dipole

"Magnetic dipole is the source of a magnetic dipole field, i.e. a field whose lowest term in a multipole expansion is a dipole term. A magnetic dipole behaves with respect to magnetic fields just as an electric dipole does with respect to electric fields. Thus, the magnetic flux density ***B*** corresponds to the electric filed, ***E***. " [5] In other words, magnetic dipole is an analogue of electric dipole that may be presented as 2 "point magnetic charges" ($\pm \boldsymbol{q_m}$) with distance ***l*** between them. [8] (It is important to mention once again, that it is only a model and each of those "point charges" does not exist independently.) Magnetic dipole may be described by a magnetic dipole moment

$$\vec{p}_m = q_m \cdot \vec{l} \quad ; \quad q_m = \rho_m \cdot V \quad ; \quad \rho_m = \nabla \cdot \vec{M} \quad (9), (10), (11)$$

where $\boldsymbol{p_m}$ is a dipole moment, $\boldsymbol{\rho_m}$ is a magnetic volume charge density, and ***M*** is magnetization. It is necessary to mention that $\boldsymbol{\rho_m}$ defines magnetostatic energy of magnetic materials. [9]

Vector of magnetic field flux B is defined as [10]:

$$\vec{B}(\vec{r}) = \mu_0 \frac{3\vec{r}\,(\vec{p}_m \cdot \vec{r}) - \vec{p}_m r^2}{4\pi r^5} = \frac{\mu_0 p_m}{4\pi r^3}(3\vec{e}_r \cos(\alpha) - \vec{e}_m) \quad (12)$$

where ***r*** is a position vector (from position of magnet dipole to position of detection of ***B***), $\boldsymbol{e_r}$ and $\boldsymbol{e_m}$ are unit vectors of ***r*** and $\boldsymbol{p_m}$, α is angle between ***r*** and $\boldsymbol{p_m}$, r and p_m are lengths of vectors ***r*** and $\boldsymbol{p_m}$, μ_0 is magnetic constant.

The length of the vector ***B*** (absolute value of magnetic field **B** on a distance r from the magnetic dipole) is given by following formula [7], [10]:

$$B(r)=\frac{\mu_0 p_m}{4\pi r^3}\sqrt{1+3\cos^2(\alpha)} \quad (13)$$

The most important part here is that B is proportional to r^{-3}.

2.3 Fluxgate magnetometer

Lorentz force is a combination of electric and magnetic forces that are acting on the point charge because of electromagnetic interaction. If a particle with charge q and velocity $\boldsymbol{v}$ is moving in presence of electric field $\boldsymbol{E}$ and magnetic field $\boldsymbol{B}$, then the total force that is acting on this particle is given by following formula [7]:

$$F_L=F_{el}+F_{mag}=q(\vec{E}+\vec{v}\times\vec{B}) \quad (14)$$

where $\boldsymbol{F_L}$ is Lorentz force, $\boldsymbol{F_{el}}$ and $\boldsymbol{F_{mag}}$ represent the influence of electric and magnetic forces.

The one of the most widespread physical phenomena that is used in magnetometers to measure the magnetic field **B**, is the Hall effect that is based on the influence of Lorentz force. But it is usually used when very high accuracy is not required. And for low-field measurements with high accuracy (up to 10^{-12} T and precision about 10^4 ppm) fluxgate magnetometers are used. [11]

During this work magnetometer had to measure low fields that had values in nT range (10^{-9} T). Thus, a fluxgate type was used. The simplest design of such a device consists of a core made from magnetic material surrounded by a pick-up coil (see Picture 1) [12]:

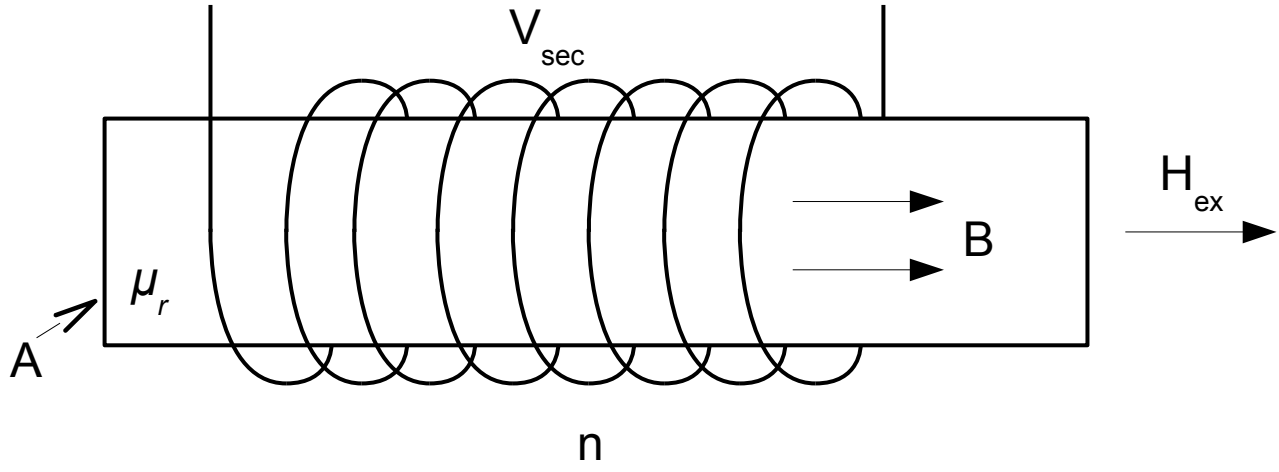

Picture 1: The simplest design of a fluxgate magnetometer

The total external magnetic filed $\boldsymbol{B_{ex}}$ (the Earth's field together with other sources of magnetic field – for more details see Chapter 2.4) along the core axis, produces a magnetic flux B in the core of

cross-sectional area A. If the relative permeability μ_r of the core material changes, then the flux in the core also changes and a voltage V_{sec} is induced in the n turns of the pick-up coil [12]:

$$V_{sec} = nA\frac{dB}{dt} \quad (15)$$

where B is proportional to $\boldsymbol{B_{ex}}$ (for relatively small values of $\boldsymbol{B_{ex}}$) and the factor of proportionality μ_a (the effective or apparent permeability) depends mostly on the core material and on the geometrical shape of the core [12]:

$$B = \mu_a B_{ex} \quad (16)$$

The field inside the core is given by

$$B = \mu_0 (H + M) \quad (17)$$

where M is the magnetization that is proportional to magnetic field H:

$$M = \chi H \quad (18)$$

where χ is a volume magnetic susceptibility and H is given by

$$H = H_{ex} - DM \quad (19)$$

where D is demagnetization factor (which is a known constant), and

$$H_{ex} = \frac{B_{ex}}{\mu_0} \quad (20)$$

According to equations (17)-(20):

$$B = \frac{\mu_r B_{ex}}{1 + D(\mu_r - 1)}; \quad \mu_r = 1 + \chi \quad (21), (22)$$

Comparing equations (16) and (21) the apparent permeability is:

$$\mu_a = \frac{\mu_r}{1 + D(\mu_r - 1)} \quad (23)$$

And inserting (21) into equation (15) gives the basic fluxgate equation [12]:

$$V_{sec} = \frac{nAB_{ex}(1 - D)\frac{d\,\mu_r}{dt}}{[1 + D(\mu_r - 1)]^2} \quad (24)$$

With proper shape and size of the core the demagnetization factor $\boldsymbol{D}$ may be so small that when the core is placed into external magnetic field, the demagnetization field → 0. In that case, according to (19) the total magnetic field inside the core will be very close to the outside magnetic field, which

simplifies the basic fluxgate equation.

In order to increase sensitivity of the detector, it is possible to use more than 1 sensing element (coil + core) in one direction. Also, it is possible to add one more coil with altering current to each sensing element. During the abcense of external magnetic field the detecting coil will receive voltage with only odd harmonics received from the electromagnetic influence of the coil with known current. The magnetization curve of core is symmetic. But in the presence of constant (or slowly changing comparing to frequency of the altering current on the coil) external magnetic field the magnetization curve of core becomes asymmetic and the voltage on detecting coil will receive also even harmonics that are proportional to projection of the magnetic field vector M to the axis of the core [10], [13].

In addition to that, it is possible to increase the number of axises of the detector by simply adding more sensing elements among the necessary axis. Picture 2 illustrates a simple model of 2D fluxgate magnetometer:

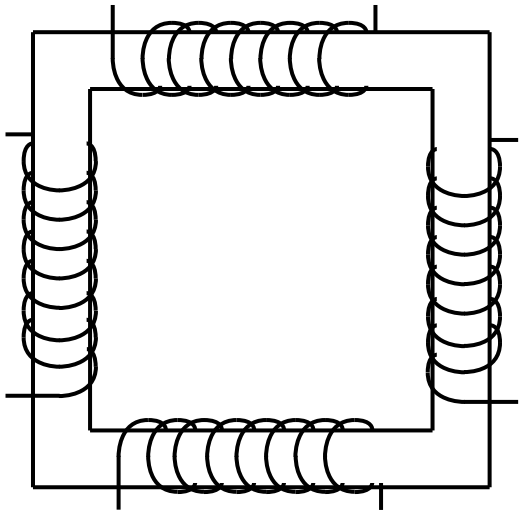

Picture 2: A simple model of 2D fluxgate magnetometer. In each sensing element a secondary coil with known altering current is absent.

In this work a 3 axis fluxgate magnetometer MAG690 (Bartington Instruments®) were used.

2.4 Magnetic field of the Earth

Earth's magnetic field, also known as the geomagnetic field, is the magnetic field that extends from the Earth's interior out into space. The magnetic field that is measured by a magnetometer on or above the Earth's surface, is actually the sum of magnetic fields generated by a variety of sources. These fields interact with each other through inductive processes. The most important of these geomagnetic fields are [14]:

1. The Earth's main magnetic field that is generated in the conducting, fluid outer core. Also known as "the core filed".
2. The field generated by magnetic minerals in Earth's crust and upper mantle.
3. The field generated by electric currents that are induced by the flow of conducting sea water through the surrounding magnetic field.
4. The combined disturbance field from electrical currents flowing in the upper atmosphere and magnetosphere, which induce electrical currents in the sea and ground.

The first 3 components of the total magnetic field of the Earth are also called as "internal" fields and their values are well known. Also, it is possible to assume that their values are constant: for example, for Estonia the change of their values between years 2010 and 2015 was less than 0.1% from their absolute values. [14]

The fourth component is also called as "external" magnetic field. It is time-varying component and together with magnetic fields from various artificial objects it forms a total noise during any magnetometric measurement. It means that the total signal of the magnetometer is given by following formula:

$$S_{total} = S_u + S_i + S_n \quad (25)$$

Where $\boldsymbol{S_u}$ is unknown signal that we want to measure; $\boldsymbol{S_i}$ is signal that is given by sum of all "internal" fields and is an already known constant; $\boldsymbol{S_n}$ is a total noise.

But still, despite various fluctuations caused by "external" magnetic field, the mean total magnetic field of the Earth is more or less constant. [14], [15]

2.5 Modeling magnetic field signal

For simplicity reasons, in this part Gaussian CGS system is being used (it means that both μ_0 and ε_0 constants are equal to 1). Actual measurements are done in SI system. Value of B may be measured in G (gauss, unit of CGS system) or in T (tesla, unit of SI), so that:

$$1\,G = 10^{-4}\,T \quad (26)$$

The distance between the magnetic dipole and the position of magnetometer is:

$$R(x,y,z)=\sqrt{x^2+y^2+z^2} \quad (27)$$

In this case, the orientation of magnetic dipole is along z-axis. So, components of magnetic field vector are given by following formulas:

$$B_x(x,y,z)=3\frac{xz\cdot p_m}{R(x,y,z)^5}$$
$$B_y(x,y,z)=3\frac{yz\cdot p_m}{R(x,y,z)^5} \quad (28), (29), (30)$$
$$B_z(x,y,z)=3\frac{z^2\cdot p_m}{R(x,y,z)^5}-\frac{p_m}{R(x,y,z)^3}$$

The total magnetic field B is:

$$B(x,y,z)=\sqrt{B_x(x,y,z)^2+B_y(x,y,z)^2+B_z(x,y,z)^2} \quad (31)$$

The coordinates are given as:

$$x(t)=v_x\cdot t+x_0$$
$$y(t)=v_y\cdot t+y_0 \quad (32), (33), (34)$$
$$z(t)=v_z\cdot t+z_0$$

where t is time, v_x, v_y, v_z are components of speed and x_0, y_0, z_0 are initial coordinates.

Picture 3 show us results of the real experiment with Kalashnikov rifle and theoretical modeling of magnet dipole:

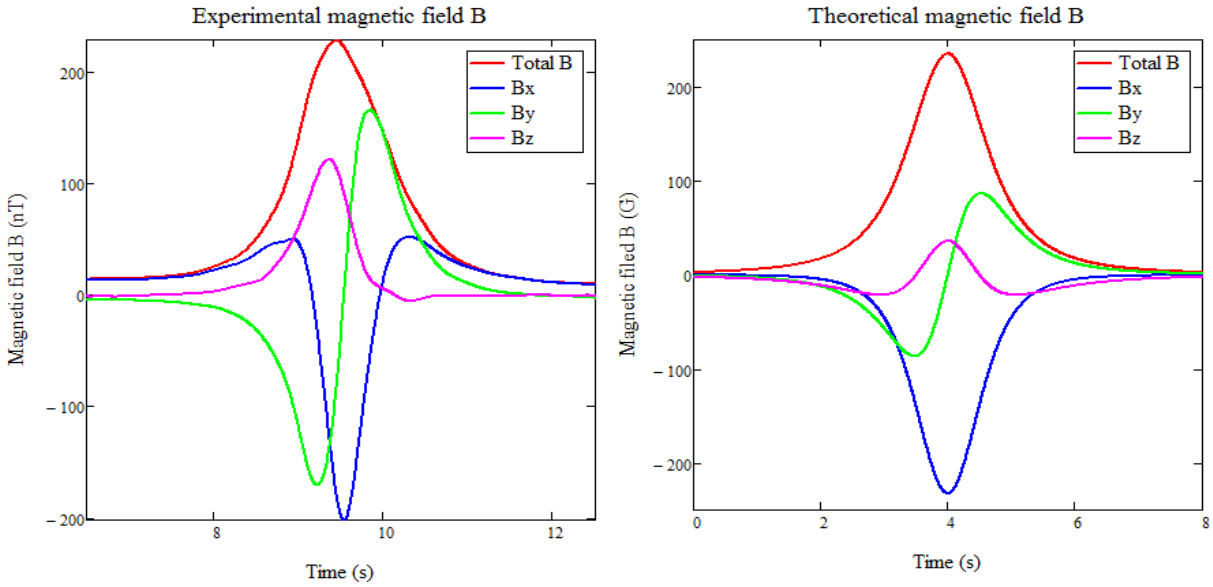

Picture 3: Result of the experiment with Kalashnikov rifle (left) and result of theoretical modelling (right). It is clear that shapes of signals are similar. The difference between magnitudes of signal among axises Y and Z may be explained by complex shape of Kalashnikov rifle.

3. Experimental work

3.1 Description of the equipment

In this work the following equipment was used:

1. Two 3 axis “Mag690-100” detectors (Bartington Instruments®), 26×22×94 mm, measuring range up to ± 100 μT, bandwidth (-3dB) > 1.5 kHz, scaling error ± 1%.
2. Special shielded cable (5 meters long) for signal transmission between sensor and data acquisition unit.
3. “Spectramag-6” data acquisition unit.
4. Special cable for power supply of data acquisition unit and both sensors.
5. USB cable for data transmission between data acquisition unit and the computer.
6. Personal computer for data storing and processing.
7. Measuring tape (maximal length – 5 m).
8. Floor surface marking.

3.2 Description of objects of interest

The following lists show a complete classification of all objects of interest:

1. Safe objects:
    1. Main object: laptop;
    2. Test objects: small magnets, large TV screen, computer screen, mobile phone, keys, wallet with coins and plastic cards, computer acoustic system, photo camera, a set of spanners and drill. They are separated from laptop because of 2 reasons: the amplitudes of their signals are much smaller (like mobile phone) or due to their size it is much easier to separate them from dangerous objects (for example, people usually do not pass through pedestrian security portal with a large TV screen or drill in their hands). Thus, main experiments (extended program) were focused on laptop, while test objects were used mostly in the end to test the False Alarm (FA) state of the system (typical experiments).

2. Dangerous objects :
    1. Not firearms:
        1. Main objects: pneumatic rifle and pneumatic pistol (extended program);
        2. Other test objects (typical experiments): kitchen knife, 2 imitations of shrapnel bomb. Those objects are also separated, because it is much harder to separate them from safe objects.
    2. Firearms:
        1. Kalashnikov rifle (deactivated);
        2. Pistols: Makarov (deactivated), USP, Colt 1911, SIG Sauer 1911, Walther P22;
        3. Taurus M/094-3 revolver.

3.3 Orientation of the detector

The magnetometer produces three independent analogue output voltages in response to the magnitude and direction of the orthogonal components of a magnetic field.

A ‘right-hand’ coordinate system is adopted. In this system, the X, Y and Z axis correspond to the thumb, first and second finger respectively of the right hand.

So, during portal measurements (two magnetometers were separated at 2.4 meters between sensors) axis X is directed towards the Magnetic North Pole and -X direction points to the South. Axis Y is directed to the East and -Y direction points to the West. Axis Z is directed down (the height decreases) and -Z direction points up (the height increases).

An alternative ‘right-hand’ orientation were used during gradiometer measurements (two magnetometers were separated about 30-40 cm between sensors). Axis X is directed towards the West and -X direction points to the East. Axis Y is directed down (the height decreases) and -Y direction points up (the height increases). Axis Z is directed to the South and -Z direction points to the North.

3.4 Experimental setup for portal measurements

There were 2 types of measurements: with magnetometers and with magnetometric gradiometers. In this chapter measurements with magnetometers are discussed. It means that the result of those measurements is the value of magnetic field B.

Picture 4 illustrates the geometry of portal experiments.

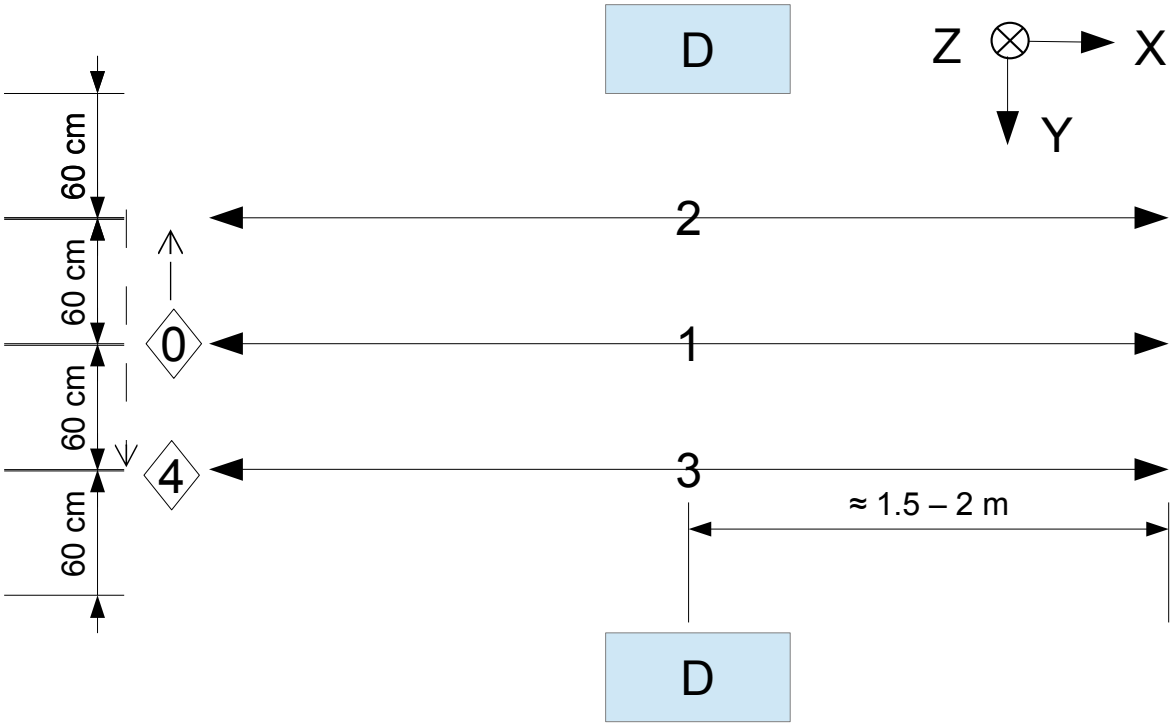

Picture 4: Experimental setup for portal measurements. ***NB!*** *The "zero" line that connects two detectors along axis Y is not shown here.*

The distance between 2 detectors is 240 cm. A straight line along Y axis that connects both detectors is being called a *"zero" line* (not shown on the picture!). Starting *position 0* is located at 200 cm along X axis and 120 cm along Y axis from any detector. Ending *position 4* is located at 200 cm along X axis from both detectors, 180 cm along Y axis from detector 1 (western) and 60 cm along Y axis from detector 2 (eastern). The distance between the floor and detectors is ~70 cm.

Detectors are connected to data acquisition unit through a shielded cable for signal transmission. The distance between detectors and data acquisition unit is >3 m. The distance between detectors and computer is >2.5 m. The maximal distance for effective signal detection of objects of interest is about 2 m.

Series of experiments were very time-consuming and it took more than 5 days to complete them all. So, every day started from calibration measurements before any real experiment. Their procedure was very simple: a person with pneumatic rifle (because the magnitude of its signal amplitude had the biggest value) stayed in position 0 for 5 seconds and then moved along the path 1 till its end. It is important to mention that those measurements were done not exactly for calibration of detectors,

but to check 2 things: the level of noise and does the work of detectors is correct. But practice showed that if the geometry of experiments was not broken during the night (position of detectors or the distance between them), then everything were always correct.

There were 3 types of experiments: *typical experiments* for all objects, *special experiments* for main objects (laptop, pneumatic rifle and pneumatic pistol) and *statistical experiments*. The aim of *typical experiments* were to get the basic information about the object. The goal of *special experiments* were to get some additional information about objects with good signal-to-background ratio, which may be (or sometimes my be not) later applied to other objects with much worse characteristics or to find out the degree of influence of orientation of the path or detectors on the result of measurement. And the aim of *statistical experiments* were to simulate real-life measurements and to check method that were developed to determine the position of the object and its safety (in other words, to answer on 2 questions: is it alarm state or not, and if yes – then where the dangerous object is located). In order to receive more reliable results, all experiments were done 3 or more times.

Also, it is necessary to mention that there were 2 types of different programs: *simple* and *extended*. *Simple program* contains only typical experiments, where object of interest had only medium height and vertical orientation. It was done for all objects of interest. But for some of them the program (mostly main objects) was extended. *Extended program* contains typical experiments with various heights and orientations of objects and/or special experiments.

Typical experiment contains:

1. Background measurement in the position 0 (5 s);
2. Moving forward (to the North) with the object of interest along the path 1 (6-8 s);
3. Background measurement in the end of the path 1 (5 s);
4. Moving backwards (to the South) with the object of interest along the path 1 (6-8 s);
5. Repeating steps 1-4 for paths 2 and 3;
6. End of experiment.

In case of laptop and pneumatic rifle typical experiments were extended: there were 7 paths instead of 3: 30, 60, 90, 120, 150, 180, 210 cm from western detector. Also, it is important to mention that during this type of experiment the orientation of the object of interest was always fixed along X, Y or Z axis and the object was always alone (total number of objects during 1 experiment was always equal to 1).

The most frequently done example of ***special experiment*** was ***rotation*** experiment:

1. Background measurement in the position 0 (5 s);
2. Moving forward (to the North) with the object of interest along the path 1 until reaching the "zero" line;
3. Background measurement (5 s);
4. Rotation of the object 90 degrees clockwise;
5. Repeating steps 3 and 4 until the object reaches original position (360 degrees in total);
6. Background measurement (5 s);
7. Rotation of the object 90 degrees counterclockwise;
8. Repeating steps 6 and 7 until the object reaches original position (360 degrees in total);
9. Background measurement (5 s);
10. Moving backwards to the starting position (to the South);
11. Background measurement (5 s) and end of experiment.

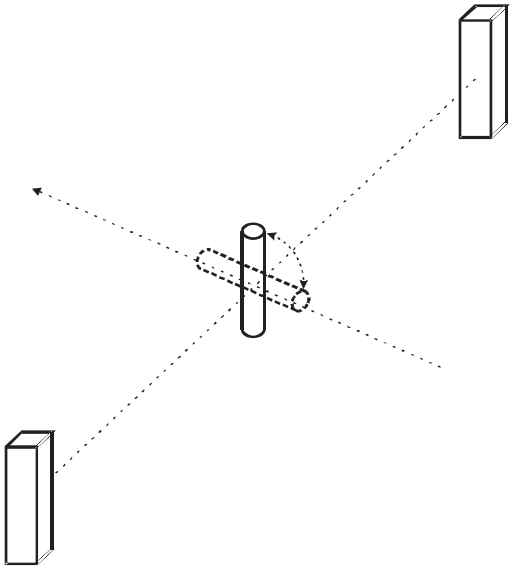

Picture 5: Rotation of the object along Y axis.

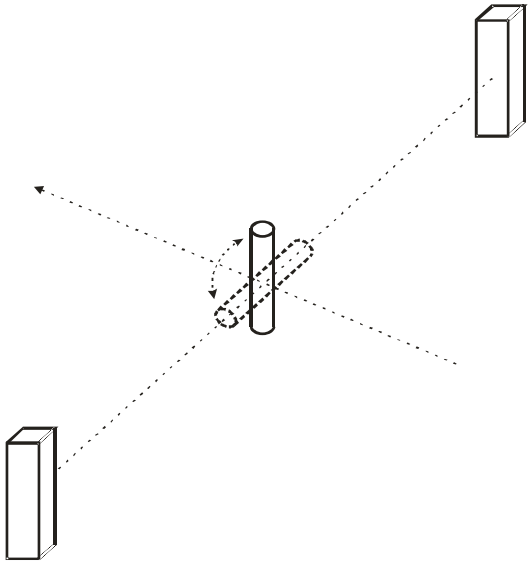

Picture 6: Rotation of the object along X axis.

Another important type of ***special experiment*** was a ***tangent*** experiment. Picture 7 shows its geometry.

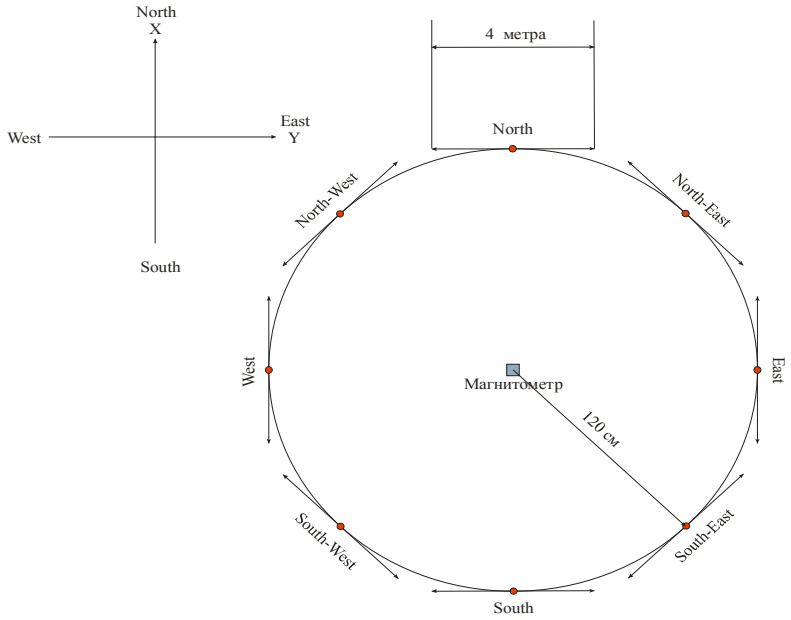

Picture 7: Experimental setup of tangent experiment.

It is clear that this time only one magnetometer was used. It was located in the center of a circle, which had 120 cm radius. The circle had 8 points: North, North-East, East, South-East, South, South-West, West, and North-West. Each point had a tangent line (to a circle) that was a path for object of interest. The total length of each path was 4 m: 2 m before the point and 2 m after the point. The procedure of each measurement was very similar to typical ones: 5 seconds of background measurements, then moving the object of interest forward till the end of the path, then once again 5 seconds of background measurements and then moving back to the beginning of the path. The aim of this experiment was to check how the direction of the Earth's field influences on results of measurements. In other words, can it *significantly* change the result of measurement or not.

The aim of *typical* and *statistical* experiments were to create a theoretical model, and the goal of *statistical* experiments was to check this model. ***Statistical experiments*** are very similar to typical ones with few differences:

1. The orientation of an object were not always fixed among X, Y or Z axis. For example, the object of interest could be orientated along XY plane, not just along X or Y axis.

2. The path was not always determined by one out of 3 main paths. For example, it could start somewhere between the beginnings of paths 1 and 2, and end at the end of path 3. But it always was a straight line.

3. Number of objects participating in one experiment were different. For example, one experiment could be only with laptop, while another experiment could be with laptop and

pneumatic pistol (laptop “attempts” to shield the pistol). Same goes to number of people that are carrying those objects: it may be up to 3 people.

3.5 Experimental setup for gradiometer measurements

A magnetometer measures a magnetic field B, providing data on its strength and direction, while gradiometer evaluates the difference between two magnetometers (sensors) measurements. In other words, the main difference between gradiometer and pair of ordinary magnetometers is that it measures not the value of magnetic field B, but *the rate of change of this value*.

Picture 8 illustrates the geometry of experiments with gradiometer. Unlike portal measurements, here the distance between detectors ***M*** (here it is along X axis) is much smaller than the distance between detectors and object ***L***. Also, it is important to notice that in order to avoid situation when one detector shields another, detector 1 was placed on 6 cm higher position than detector 2 (See Appendix 1). The height of each of them is 22 mm, so space between the bottom of detector 1 and the top of detector 2 along Y axis is 38 mm. The distance between the floor and detector 2 was the same (70 cm).

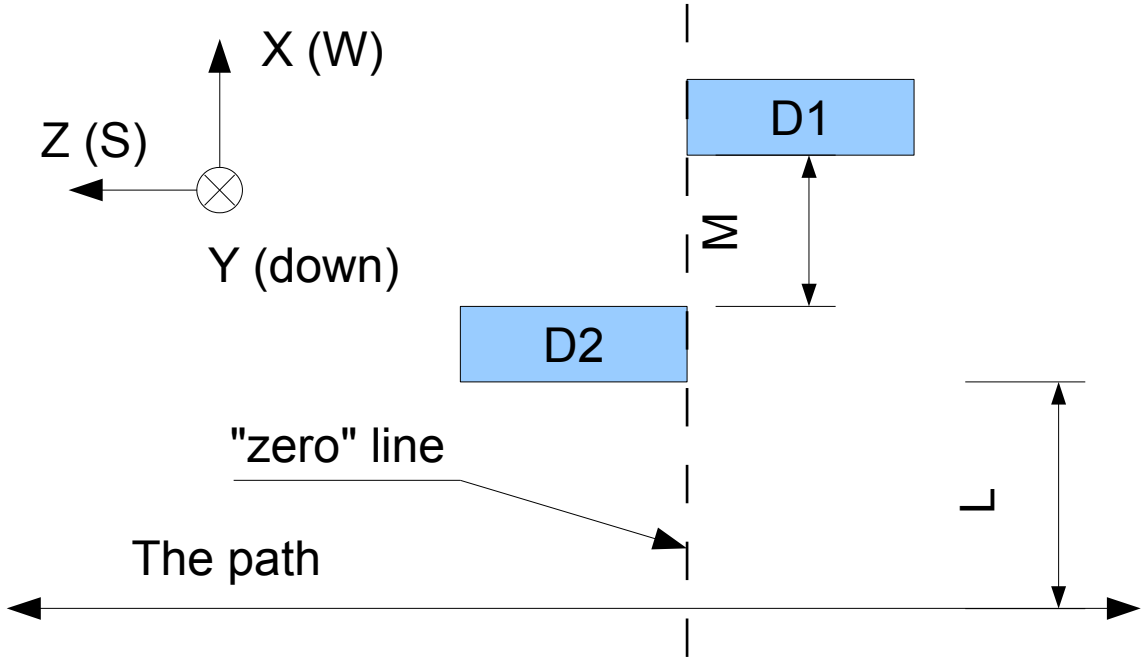

Picture 8: Experimental setup for gradiometer experiments.

Due to lack of available detectors, it was not possible to make experiments with portal gradiometer. In that case, it is necessary to have at least 4 detectors: 2 from each side of the portal. So, the aim of gradiometer experiment was to compare dependencies of the signal from single magnetometer and

gradiometer on distance from the object and their signal-to-noise ratios.

As it was in (12) and (13), the value of magnetic field B in a point that is located on distance r from a magnetic dipole is directly proportional to r^{-3}. Knowing that

$$\frac{d\left(r^{-3}\right)}{dr} = -3\frac{1}{r^4} \quad \rightarrow \quad \frac{dB}{dr} \sim \frac{1}{r^4} \quad (35), (36)$$

it is possible to say that the value of gradiometer measurement is directly proportional to r^{-4}. It means that all measurements become more sensitive to distance, so to get precise results, the number of different L was increased comparing with number of portal measurements (15 versus 7). The following L were measured: 30, 45, 60, 75, 90, 105, 120, 135, 150, 165, 180, 195, 210, 225, 240 cm.

The procedure of experiment was somehow similar to both *typical* and *special rotational* portal measurements:

1. Background measurement in the beginning of the chosen path (more than 2 m towards the South from "zero" line, 5 s);
2. Moving forward (to the North) with the object of interest along the chosen path (3-4 s) until the object reaches "zero" line;
3. Signal measurement in the point where the chosen path is being crossed by zero line, object is not being moved! (5 s);
4. The end of experiment. But sometimes it was also extended (to get data from reverse object orientation):
5. Moving forward (to the North) with the object of interest along the chosen path (3-4 s) until the end of the path;
6. Repeating steps 1-4 while moving in opposite direction (from end of the path to its beginning)
7. Final background measurement in the beginning of the path (5 s);

A small pause in the middle of the path was necessary to fix the position of the object as precisely as possible. The difference between neighboring L was 15 cm, so it was measured as the distance between the center of the fixed object and the side of detector that was the closest to the object.

Due to limited time, gradiometer measurements were done only for pneumatic rifle objects. But it still allows to compare received results with results from single detector measurements.

3.6 Experiments with real weapons

The aim of experiments with weapons was to measure magnetic properties of real weapons and to check the work of the the portal system that was developed using results of portal experiments with safe objects.

Experiments with real firearms were made only according to *typical extended* portal program (without gradiometer): for each weapon there were 3 axis measurements (along X, Y and Z axises) + 1 additional Z-axis measurement (for more details see Appendix 2, Appendix 3). For all experiments with weapons the distance between floor and center of weapon was ~1 m (medium height). Orientation of detectors was the same as during ordinary portal experiments (X – North, Y – East, Z – down).

In addition to that, Kalashnikov rifle participated in rotation experiments.

4. Data processing and results

4.1 Signal filtering

There are two main types of filters, namely finite impulse response (FIR) and infinite impulse response (IIR). In this work, the classical ***IIR Butterworth low-pass filter*** was used. Comparing with other classical IIR filters (Chebyshev and Elliptic), it has the poorest frequency selectivity, but it is the simplest to design. [16]

Any digital filter has its own impulse response function. It is an output of the system, when the input is a very brief signal, called impulse. The ideal impulse has a shape of a delta function that may be defined as [17] :

$$\delta = \begin{Bmatrix} \infty, x = 0 \\ 0, x \neq 0 \end{Bmatrix}; \quad \int \delta(x)\,dx = 1 \quad (37), (38)$$

In case of digital IIR, impulse response function *h(n)* has an infinite number of non-zero samples (*n* – number of sample). For a general IIR filter, $h(n) \neq 0$ only for $N_0 \leq n \leq \infty$, N_0 is a positive integer.

The general frequency response (or transfer function in frequency domain) of any IIR filter $H(\omega)$ is a rational function, which means that it is a ratio of two finite-degree polynomials, where A is an input signal in frequency domain ω and B is an output signal in frequency domain ω [16]:

$$H(\omega) = \frac{B(\omega)}{A(\omega)} = e^{-j\omega N_0} \frac{\sum_{k=0}^{M} b_k e^{-j\omega k}}{\sum_{k=0}^{N} a_k e^{-j\omega k}} \quad (39)$$

The magnitude-squared function of an *N-th* order Butterworth lowpass filter is given by following formula [16]:

$$|H(j\Omega)|^2 = \frac{1}{1 + \left(\frac{\Omega}{\Omega_c}\right)^{2N}}; \qquad \Omega = K \cdot \tan\left(\frac{\omega}{2}\right) \quad (40), (41)$$

Where K is design parameter that can be used to control the location of the designed cut-off frequency.

In this work, the order of the filter $N=6$, sample rate is 200 Hz, and cut-off frequency is 3.667 Hz.

Picture 9 illustrates typical frequency spectra of raw (not filtered) signal. There is a clear noise peak at 50 Hz and another peak at 0-5 Hz region that contains both noise and useful signal.

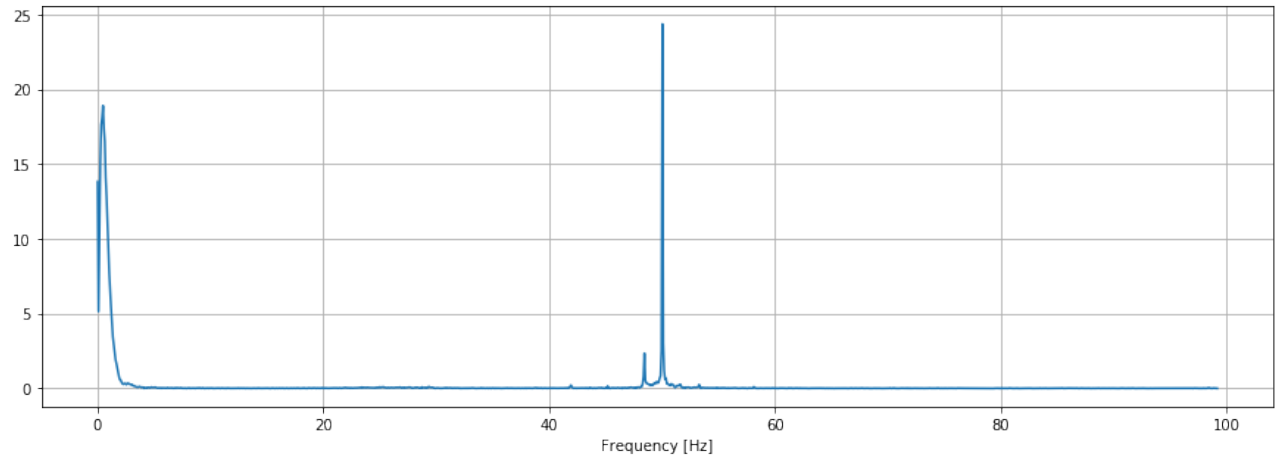

Picture 9: Frequency spectra of single typical measurement.

Picture 10 illustrates frequency response of the designed filter:

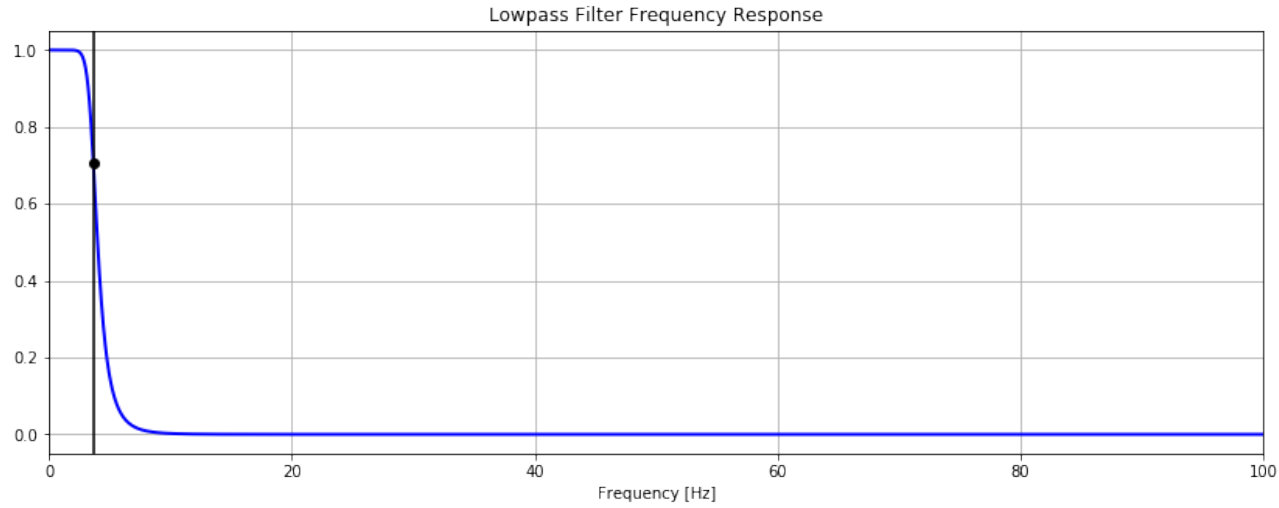

Picture 10: Frequency response of the filter.

Picture 11 illustrates the work of the designed filter with signal from a real weapon (Walther P22). It is clear that despite a very low (much less than 1) signal-to-noise ratio, it is still possible to detect a peak. The results of long-term experiments showed that a part of useful signal gets lost during the filtration process. The value of the lost signal is directly proportional to the amplitude of the background noise, so during measurements with the highest noise level (up to 60 nT) the results were worse than during measurements with lowest noise level (up to 15 nT, like on the picture below).

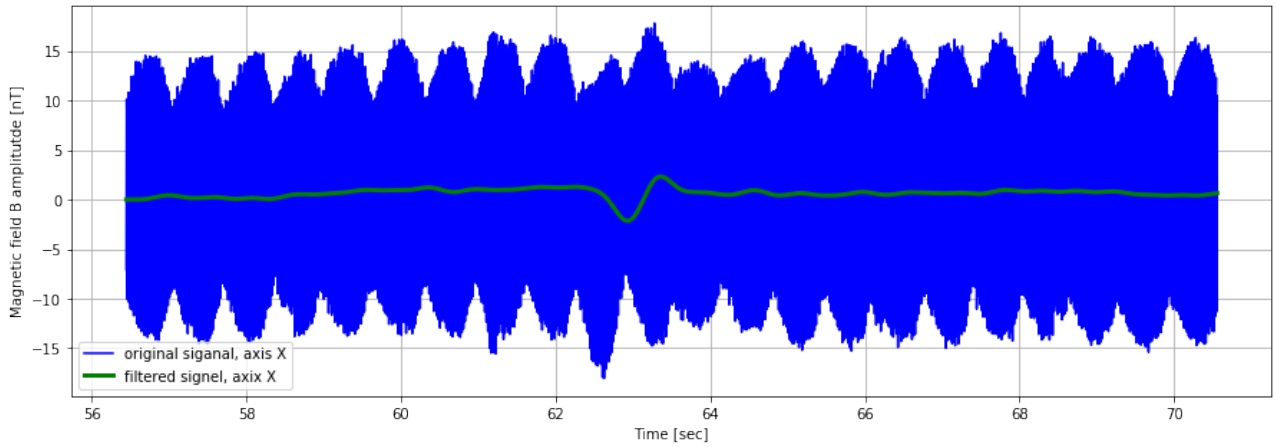

Picture 11: Example of raw and filtered signal of Walter P22.

4.2 Processing and results of filtered data

The result of successful data filtering is a pure signal almost without any noise. Now it is possible to make calculations and analyse results.

4.2.1 Special experiments

The typical result of **rotation experiments** is being shown in the Picture 12:

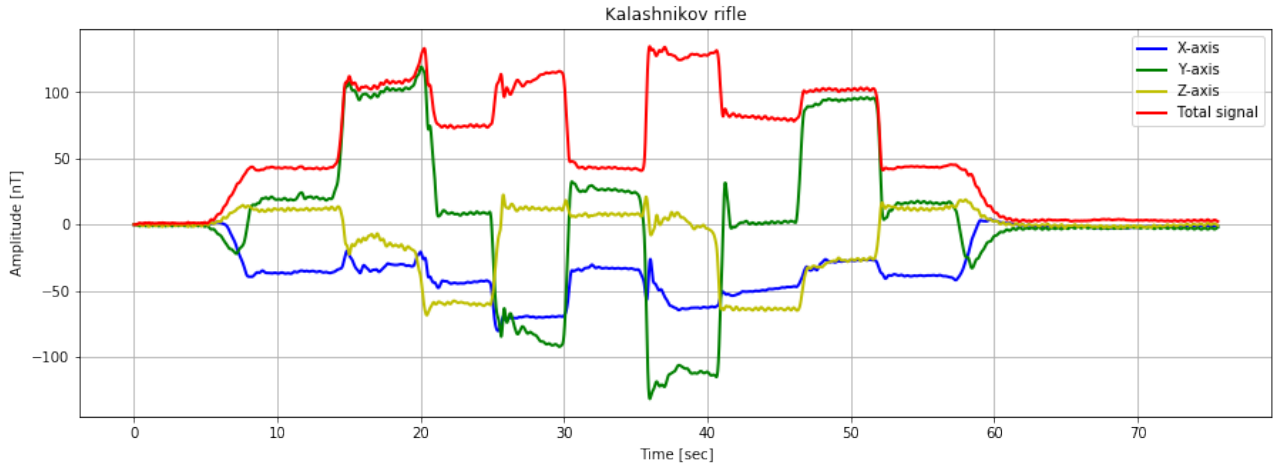

Picture 12: Rotation (along axis X) experiment with Kalashnikov rifle.

NB! Here is alternative orientation of detectors (axis X is directed towards the West, axis Y is directed down, axis Z is directed to the South). It means that a “zero” line is parallel to axis X here and to axis Y during ordinary portal experiments.

The results of experiments have shown that the change of the amplitude due to rotation of the object does exist, but it is not very high: **~20% from the mean value of non-rotating objects**.

Picture 13 illustrates the result of the **tangent** experiment with pneumatic rifle.

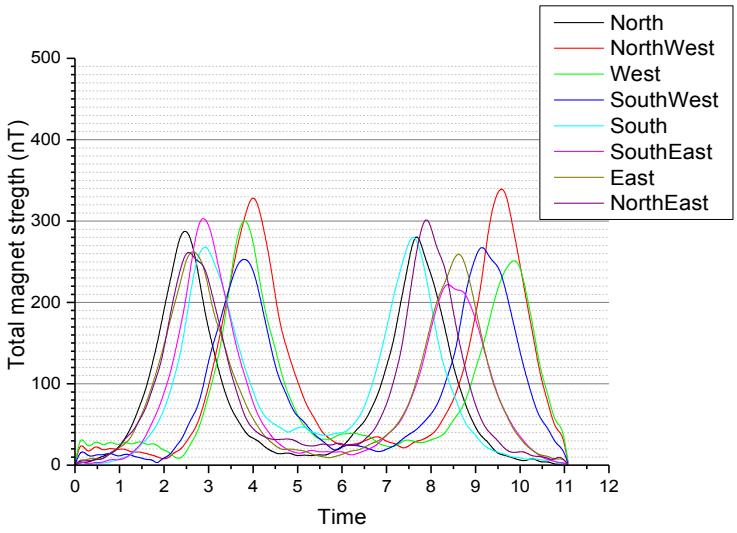

Picture 13: Results of the tangent experiment with pneumatic rifle.

The results of this experiment are clear:

1. The difference between various directions of the path does exist, but it is not significant comparing with the average value of 270 nT (the difference between the average and the maximum or minimum is less than 20%).

2. The difference between moving the object in one direction and then moving in the opposite direction (the first and the second peaks of any path) also does exist, but it is also insignificant (less than 20%).

4.2.2 Typical and statistical portal experiments

First of all, it is necessary to get the value of signal amplitude. There are various ways for simple automatic peak detection and they are necessary for the real security portals, but in this work it is possible to assume that almost all noise is already filtered and that the possible position of the peak on a time scale is known. It means that it is possible to use the simplest way of the peak detection – to simply find the maximal value of signal for certain time period.

When all 3 signal amplitudes (A_X, A_Y and A_Z) for for both detectors are found, it is possible to find the total signal amplitude for each detector (A_1 and A_2):

$$A = \sqrt{A_x^2 + A_y^2 + A_z^2} \quad (42)$$

In order to get better result, each experiment was done more than 3 times. Due to that it is possible to find the mean value of A: we sum up all amplitudes that share the same path with each other and then divide it on their total number (N). Due to absence of information about B-type uncertainty, we may use only experimental standard deviation of the mean (A-type uncertainty) to form total uncertainty. Also, we may say that degree of freedom ν is equal to N – 1. [18]

$$A=\frac{\sum_{i=1}^{N} A_i}{N}; \qquad u_A(A)=\sqrt{\frac{\sum_{i=1}^{N}(x_i-\bar{x})^2}{N(N-1)}} \quad (43), (44)$$

When both amplitudes are found, it is possible to find the value of ***R*** that is given as

$$R=\frac{A_2}{A_1}; \qquad u_C(R)=\sqrt{\left(\frac{d(R)}{dA_1}u_A(A_1)\right)^2+\left(\frac{d(R)}{dA_2}u_A(A_2)\right)^2} \quad (45), (46)$$

$$\nu_{eff}=\frac{u_C(R)^4}{\frac{\left(\frac{d(R)}{dA_1}u_A(A_1)\right)^4}{N-1}+\frac{\left(\frac{d(R)}{dA_2}u_A(A_2)\right)^4}{N-1}} \quad (47)$$

where u_C is combined uncertainty and ν_{eff} is effective degree of freedom for R [18]. Effective degree of freedom is necessary to obtain expanded uncertainty (U) that is giving a coverage interval for sigma with specified probability [18]:

$$U(R)=t(\nu_{eff})\cdot u_C(R) \quad (48)$$

In this case, t is coverage factor of Student's t test, that depends on effective degree of freedom and specified probability (here p = 95%).

Picture 14 illustrates the dependence of the R on distance between detector 1 and the object, when the object was crossing the “zero” line (detector #1 is at point 0 cm, detector #2 – at point 240 cm).

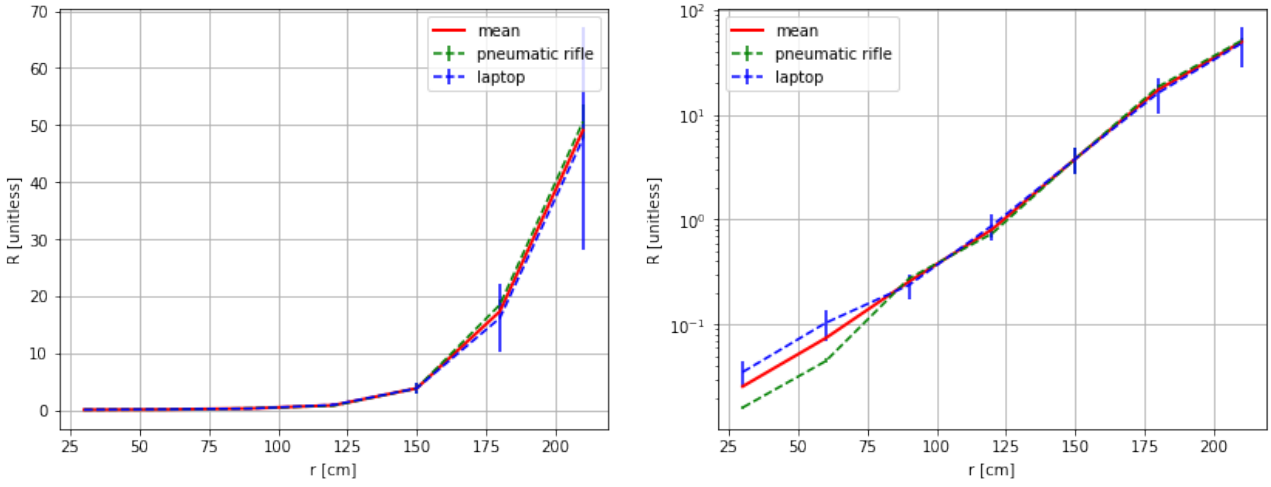

Picture 14: Dependence of R on r.

It is clear that R has a close, but not equal to 1 value at distance 120 cm (same length from both detectors). This may be explained, because during all experiments the signal from detector 2 contained more noise (it had lower signal-to-noise ratio) than from detector 1 (the filter cannot erase the whole noise without decreasing the amplitude of the signal). And the reason for this is that second detector was closer to electrical lines of the building, where whole experimental work was done.

Also, it is possible to see that when the distance is less than 90 cm from the first detector (more than 150 cm from the second one) or more than 150 cm (less than 90 cm from the second one) the expanded uncertainty (with 95% probability) of the result increases. This may be explained by 2 reasons. First of all, the sensor inside the detector and the object of interest are not just a points with zero volume, the they have their own non-zero size. And when the distance between sensor and the object becomes small enough (comparing with sizes of both object and sensor), then it is necessary to take the shape of the object and/or sensor into account. And secondly, when the distance between the object and detector increases, the signal-to-noise ratio decreases. It happens, because the amplitude of the peak decreases, while the noise is the same.

And the most important thing is that the dependence of R on r is the same for all ferromagnetic materials (assuming that magnetic dipole moment $\boldsymbol{p_m}$ is constant when that object is passing through the portal). It means that the dependence of R on r that was received during experiments with pneumatic pistol (not shown on the graph), pneumatic rifle and laptop may be used for estimation of position of any ferromagnetic object with large enough magnetic dipole moment.

As it is shown in (13), the length of the magnetic field vector $\boldsymbol{B}$ depends not only on geometrical properties of the setup (like distance r or angle α), but also on properties of the material of object, like magnetic dipole moment $\boldsymbol{p_m}$. If we assume that during the moment (up to 0.2 seconds) when object is passing through the portal (moment, when we get the amplitude signal):

1. the orientation of object of interest and its speed are constant,
2. the path of the object is a straight line that is perpendicular to the plane of the portal,
3. magnetic properties of the object are constant,

then it is also possible to assume that α and $\boldsymbol{p_m}$ are constants. Then, it is possible to say that

$$B(r)=\frac{C}{r^3}; \qquad C=c_1 p_m \quad (49), (50)$$

where C (magnetic signature) and c_1 are also constants. Knowing that magnetic signature contains p_m, it is possible to say that magnetic signature describes magnetic properties of the object and its dimension is [T·m^3].

It means that if the security portal detects a peak with high enough amplitude, it is possible to receive values of magnetic field B and distance r. After that, by multiplying B and r^3 we receive the

value of magnetic signature that is proportional to magnetization M of the object:

$$M = \frac{dp_m}{dV} \quad \rightarrow \quad M \sim p_m \quad (51), (52)$$

And finally, if C is greater that certain limit, then the whole portal system informs the security workers to check a person, who was in a position r (point where the path of this person crosses "zero" line) while walking through the portal. Statistical experiments showed that it is possible to separate pneumatic rifle from all safe objects with low enough false alarm rate if the maximal "safe" amplitude is **100 nT·m^3** and detect the position of dangerous object with **±20 cm** accuracy.

The received data was used to write a special program in Matlab based on this algorithm by other members of APSTEC Systems Ltd. The input of this program is real-time data from magnetometer and an output are 2 signals: "safe" and "danger".

4.2.3 Experiments with gradiometer

It is necessary to mention once again that the aim of experiments with gradiometer was to compare dependencies of the magnetic field B and its gradient of real objects on distance and dependencies of their signal-to-noise ratios on distance.

The results of gradient measurements were quite unexpected. Picture 15 shows the comparison of magnitude of magnetic field B that is detected by detector 2 with gradient of field B between 2 sensors (difference between 2 amplitudes of magnetic field B divided on the distance between 2 detectors: $(A_1 - A_2)/20$ cm).

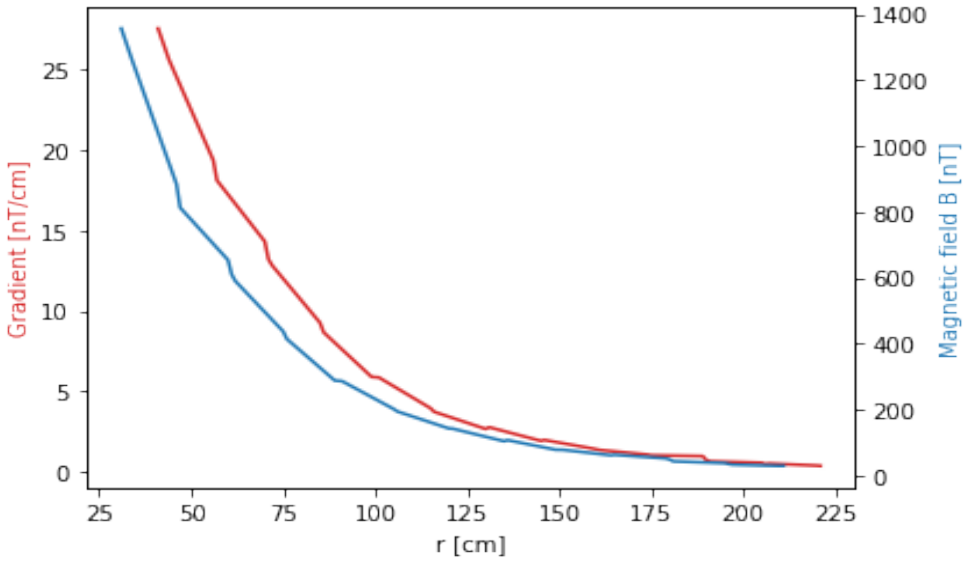

Picture 15: Comparison of magnetic field B with its gadient.

The true distance between detector and the object of interest begins not from detector 2 (that is closer to the object), but from the sensor that is located in the center of detector. However, this fact gives an error about ±1 cm, which may be neglected in calculations. The shift between distances comes from the fact that the geometrical center of gradiometer is shifted on ~11 cm from the censor of detector #2 and is located between detectors.

Picture 15 shows that the shape of the curve of the gradient is very similar to the shape of the B curve. This may be explained by the size of the object: the length of pneumatic gun that was used during this experiment is ~70 cm, so on the distances less than 1 m it may be impossible to correctly describe the gradient of the magnetic field that is made by this rifle without taking into account its shape and size.

However, the same experiment showed that gradiometer does have its own advantage comparing with ordinary detector.

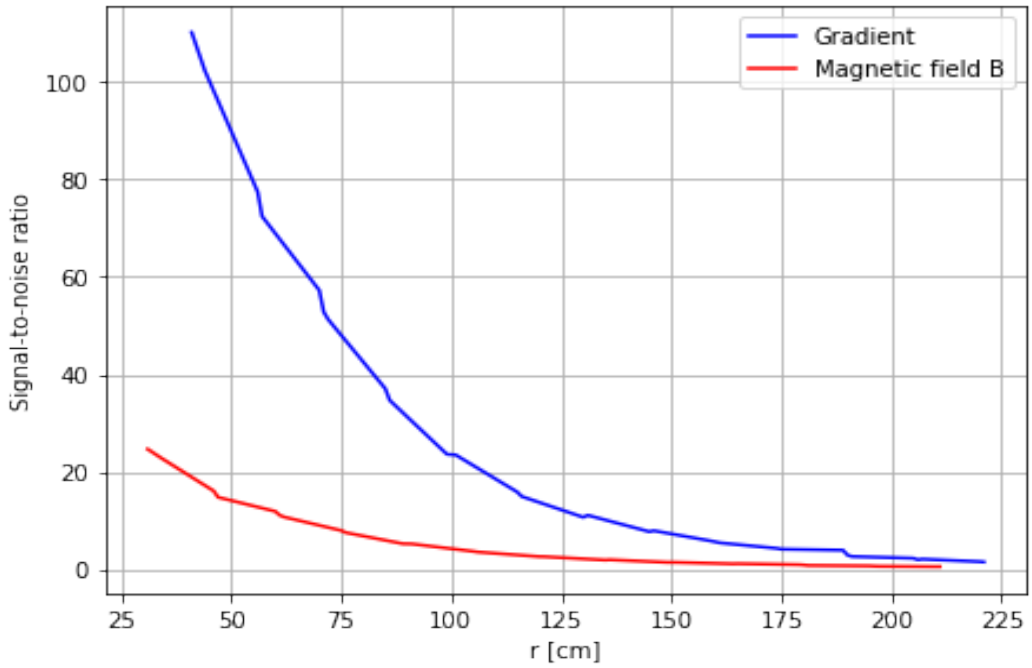

Picture 16: Comparison of signal-to-noise ratio of gradiometer and single detector.

Picture 16 illustrates the dependence of signal-to-noise ratio (SNR) of magnetometer and magnetometric gradiometer on distance. It is crystal clear that SNR of gradiometer is much better than SNR of single magnetometer. It happens due to the fact that the noise has approximately constant value, while signal does not. Thus,

$$B_n \approx const \neq 0 \quad \rightarrow \quad \frac{dB_n}{dr} \approx 0 \quad (53), (54)$$

where B_n is a noise signal. So, it is highly recommended to use 2 magnetometric gradiometers (4 detectors in total) instead of ordinary magnetometers (2 detectors in total) for design of pedestrian

security portal.

4.2.5 Experiments with real weapons

As it was already mentioned in experimental part, the aim of experiments with real weapons was to measure magnetic signature of real weapons and to check the work of portal system that was developed using results of portal measurements with ordinary objects.

The following table shows results of experimentally measured magnetic signature ($nT \cdot m^3$) and its expanded uncertainty (95% probability) of real weapons and some ordinary objects:

Object of interest	Magnetic Signature	Uncertainty
Kalashnikov	82	10
Makarov	17	4
USP	6	4
Colt 1911	13	5
SIG Sauer 1911	10	5
Walther P22	17	6
Taurus M/094-3	10	5
Laptop	59	8
Mobile phone	10	4
Pneumatic rifle	273	30
Pneumatic pistol	8	4

The laptop was chosen as a main “safe” object, because it had the strongest signal among them (except big TV screen and drill). Now it is clear that:

1. Automatic weapons, such as Kalashnikov rifle, may be separated from from ordinary objects. However, due to relatively small difference between laptop and Kalashnikov rifle it would be necessary to find the most optimal balance between false alarm rate and probability that automatic weapon will pass through the portal unnoticed. In other words, do determine proper the minimal value of magnetic signature for “alarm state”.

2. It would be almost impossible to separate small weapons like pistols from safe objects with current portal search methodics without significantly increasing false alarm rate.

5. Conclusion

The whole experimental work and data processing of this thesis may be divided on 3 parts:

1. Study of various effects that are based on existence of magnetic field of the Earth and which may occur during work of security portal (*special experiments*);

2. Study of magnetic properties of various objects (including weapons), measuring the dependence of *R* on *r* for portal detection system (*typical experiments*) and testing it (*statistical experiments*);

3. Comparing dependences of signal of gradient of the magnetic field B and the magnetic field B itself and their SNR on distance between the object of interest and gradiometer/magnetometer for possible future modification of security portal.

The results are:

1. Various effects do influence on results of measurements but their impact is not significant.

2. The magnetometer portal system is able to successfully separate automatic weapons from most of ordinary objects and to measure the position of a dangerous object with accuracy ±20 cm.

3. The gradient measurements showed that this configuration significantly decreases SNR. Thus it is highly recommended to choose configurarion of pedestrian security portal based on magnetometric gradiometer.

This work was a small part of long designing process of a real portal security system that could detect automatic weapons without special preparation of people (they do not need to take off all metal objects from themselves) that are passing through the portal. The whole work was done in collaboration with APSTEC Systems Ltd, that plans to combine this security portal with Human Security Radar system (HSR).

HSR itself is based on a scanning with active centimeter-range radio waves and is able to find people carrying threat dielectric objects and/or metallic objects under clothes or in backpacks. “HSR operates remotely, covertly and in real time without slowing down the people flow. Coordinates of the located potentially suspicious person and hazardous objects on its body are sent to a higher-level security system, or can be optionally superimposed on an ordinary video image.” [3]

Together with magnetometer portal that can separate automatic weapons (like Kalashnikov rifle) from ordinary objects (like laptops, mobile phones and keys) **and gamma detector** that can separate medical and industrial sources of gamma radiation from dangerous ones (including quantitative separation – if medical gamma radiation is too intensive it will also give an alarm) **HSR becomes a flexible multi-threat detection system** that can be set up to simultaneously detect

dielectrics (e.g. explosives), metallic objects (automatic weapons, shrapnel), as well as radioactive and nuclear materials. [2], [3], [4]

References

[1] Boris Y. Kapilevich et al. *Non-Imaging Microwave and Millimetre-Wave Sensors for Concealed Object Detection*, CRC Press, ISBN-13:978-1-4665-7719-0, eBook-PDF, (2015).

[2] Andrei Kovaljov, *Development of method for determination of minimal detection ability of bismuth germanium oxide gamma detector*, Bachelor's thesis, University of Tartu (2016)

[3] Andrey Kuznetsov et al, *Extending Security Perimeter and Protecting Crowded places with Human Security Radar*, APSTEC Systems, Tallinn (2015)

[4] Viktor Meshcheryakov et al, *Human Security Radar: the brave new world of non-cooperative inspection*, APSTEC Systems, Tallinn (2018)

[5] L. Coleman et al, *Dictionary of physics*, Antony Rowe Ltd, Chippenham, UK, vol 3 (2004)

[6] M. G. Brik, I. Sildos, V. Kiisk, *Introduction to spectroscopy of atoms, molecules and crystals,* Tartu University Press, Tartu (2008)

[7] S. G. Kalashnikov, *Electricity*, Nauka, Moscow (1985) / С. Г. Калашников, *Электричество*, Наука, Москва (1985)

[8] А. М. Прохоров и др., *Физическая энциклопедия*, издательство «Советская энциклопедия», Москва, том 1, с. 628-629 (1990)

[9] А. М. Прохоров и др., *Физическая энциклопедия*, издательство «Советская энциклопедия», Москва, том 2, с. 686 (1990)

[10] Ю. С. Осипов и др., *Большая российская энциклопедия*, издательство «Большая российская энциклопедия»

https://bigenc.ru/physics/text/2153456

https://bigenc.ru/technology_and_technique/text/4710038

[11] I. S. Grant, W. R. Phillips, *Electromagnetism*, John Wiley & Sons, Chichester, UK, Second edition, pp. 123-125, 247 (1999)

[12] F. Primdahl, *The fluxgate magnetometer*, Journal of Physics: Energy, Vol. 12, Number 4, April (1973)

[13] J. V. Afanasjev et al, *Ways of measurements of parameters of magnetic field*, Energia, Leningrad (1979) / Ю. В. Афанасьев и др., *Средства измерений параметров магнитного поля*, Энергия, Ленинград (1979)

[14] A. Chulliat et al, *The US/UK world magnetic model for 2015-2020: Technical Report*, National Geophysical Data Center, NOAA, pages 1-2, 52.

https://data.nodc.noaa.gov/cgi-bin/iso?id=gov.noaa.ngdc:WMM2015_Technical_Report

[15] J. Guyodo, J.-P. Valet, *Global changes in intensity of the Earth's magnetic field during the past 800 kyr*, Nature, vol 399, 249-252 (20 May 1999)

[16] Vijay K. Madisetti, *The digital signal processing handbook*, CRC Press & IEEE Press, USA,

pp. 11-6, 11-7, 11-32, 11-32 (1998)

[17] Hwei P. Hsu, *Signals and Systems*, McGraw-Hill Companies Inc, USA, p. 56 (1996)

[18] Rein Laaneots, Olev Mathiensen, Jurgen Riim. *Metroloogia. Õpik kõrgkoolidele*, pp. 122, 172, 179, 186-188 (TTÜ kirjastus, Tallinn 2012)

Lihtlitsents lõputöö reprodutseerimiseks ja lõputöö üldsusele kättesaadavaks tegemiseks

Mina, Andrei Kovaljov,

1. annan Tartu Ülikoolile tasuta loa (lihtlitsentsi) enda loodud teose MAGNETOMETRIC METHODS FOR DETECTION OF FERROMAGNETIC OBJECTS, mille juhendaja on Alan Henry Tkaczyk,

    1. reprodutseerimiseks säilitamise ja üldsusele kättesaadavaks tegemise eesmärgil, sealhulgas digitaalarhiivi DSpace-is lisamise eesmärgil kuni autoriõiguse kehtivuse tähtaja lõppemiseni;

    2. üldsusele kättesaadavaks tegemiseks Tartu Ülikooli veebikeskkonna kaudu, sealhulgas digitaalarhiivi DSpace´i kaudu kuni autoriõiguse kehtivuse tähtaja lõppemiseni.

2. olen teadlik, et punktis 1 nimetatud õigused jäävad alles ka autorile.

3. kinnitan, et lihtlitsentsi andmisega ei rikuta teiste isikute intellektuaalomandi ega isikuandmete kaitse seadusest tulenevaid õigusi.

Tartus, 04.06.2018

Appendix

Appendix 1: Gradiometer setup

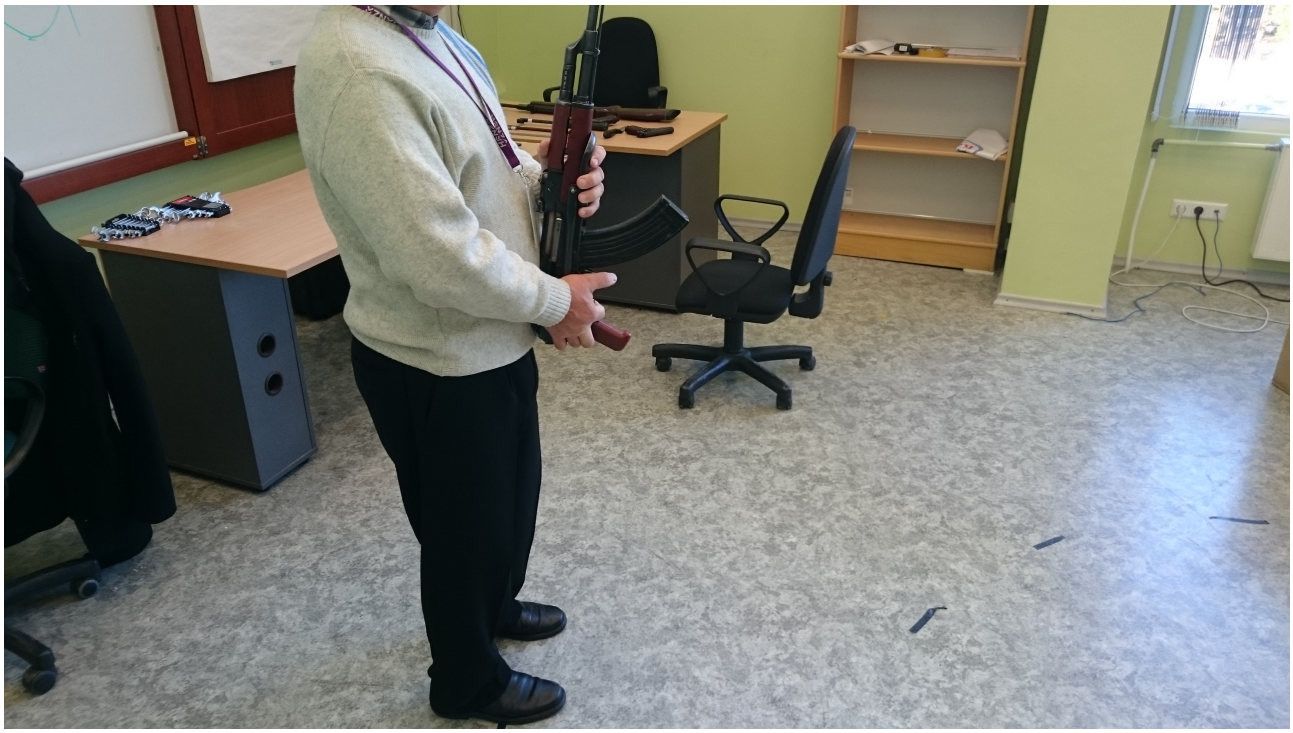

Appendix 2: Kalashnikov among Z-axis up.

Appendix 3: Kalashnikov among Z-axis down